Coulombic Forces in Protein−RNA Interactions: Binding and Cleavage by Ribonuclease A and Variants at Lys7, Arg10, and Lys66[†]

Barbra M. Fisher,[‡] Jeung-Hoi Ha,[‡,§] and Ronald T. Raines*[,‡,||]

Departments of Biochemistry and Chemistry, University of Wisconsin−Madison, Madison, Wisconsin 53706

Received April 1, 1998; Revised Manuscript Received June 30, 1998

ABSTRACT: The interactions between bovine pancreatic ribonuclease A (RNase A) and its RNA substrate extend beyond the scissile P−$O_{5'}$ bond. Enzymic subsites interact with the bases and phosphoryl groups of the bound substrate. Those residues interacting with the phosphoryl group comprise the P0, P1, and P2 subsites, with the scissile bond residing in the P1 subsite. Here, the function of the P0 and P2 subsites of RNase A is characterized in detail. Lys66 (P0 subsite) and Lys7 and Arg10 (P2 subsite) were replaced with alanine residues. Wild-type RNase A and the K66A, K7A/R10A, and K7A/R10A/K66A variants were evaluated as catalysts for the cleavage of poly(cytidylic acid) [poly(C)] and for their abilities to bind to single-stranded DNA, a substrate analogue. The values of k_{cat} and K_m for poly(C) cleavage were affected by altering the P0 and P2 subsites. The k_{cat}/K_m values for poly(C) cleavage by the K66A, K7A/R10A, and K7A/R10A/K66A variants were 3-fold, 60-fold, and 300-fold lower, respectively, than that of wild-type RNase A. These values indicate that the P0 and P2 subsites contribute 0.70 and 2.46 kcal/mol, respectively, to transition-state binding. Binding experiments indicate that the P0 and P2 subsites contribute 0.92 and 1.21 kcal/mol, respectively, to ground-state binding. Thus, the P0 subsite makes a uniform contribution toward binding the ground state and the transition state, whereas the P2 subsite differentiates, binding more tightly to the transition state than to the ground state. In addition, nucleic acid binding to wild-type RNase A is strongly dependent on NaCl concentration, but this dependence is diminished upon alteration of the P0 or P2 subsite. The logarithm of K_d is a linear function of the logarithm of $[Na^+]$ over the range 0.018 M ≤ $[Na^+]$ ≤ 0.14 M, with $\partial \log K_d/\partial \log [Na^+] = 2.3 \pm 0.1$, 1.8 ± 0.1, 1.4 ± 0.1, and 0.9 ± 0.2 for nucleic acid binding to wild-type RNase A and the K66A, K7A/R10A, and K7A/R10A/K66A variants, respectively. Similar experiments with NaF and the wild-type enzyme yield $\partial \log K_d/\partial \log [Na^+] = 2.0 \pm 0.2$, indicating that the anion makes only a small contribution to nucleic acid binding. Together these data provide a detailed picture of the contributions of Coulombic interactions to binding and catalysis by RNase A, and illuminate the general role of Coulombic forces between proteins and nucleic acids.

The viability of organisms relies on protein−nucleic acid interactions. Somatic cells undergo division, a process that requires the replication and transcription of DNA and the translation of RNA. These chemical reactions are catalyzed and regulated by proteins.

Recognition of nucleic acids by proteins involves both sequence-dependent and sequence-independent interactions. Sequence-dependent interactions usually arise from direct contacts between the protein and the exposed edges of nucleic acid bases, as in the major groove of B-DNA. These contacts may involve hydrogen bonds or van der Waals interactions between the protein and the nucleic acid. For example, the amino group of a cytosine base can form a hydrogen bond with the side chain of a threonine residue or with a main-chain carbonyl group. Sequence-dependent malleability of duplex DNA or RNA also results in structural features that are recognized by proteins. These features include kinks, bends, and twists in the duplex strands, and melting of base pairs (*1*, *2*). Protein folding transitions and other protein conformational changes are also coupled to DNA binding (*3*). Attractive forces between the anionic phosphoryl groups of nucleic acids and the cationic side chains of proteins are a primary source of sequence-independent interactions between these biopolymers.

Sequence selectivity can be quantitated as the difference between the binding free energies for the sequence-dependent and sequence-independent components of the protein−nucleic acid complex (*4*). This selectivity can vary widely. For example, a single base-pair change in a critical operator sequence can reduce its affinity for a repressor protein by more than 10^3-fold (*5*), and a similar change in the recognition site of an endonuclease can eliminate all detectable enzymatic activity (*6*). In these systems, sequence selectivity is critical, as formation of a specific complex is a prerequisite for biological function. Still, not all nucleic acid-binding proteins employ strict sequence specificity. The β-subunit of *Escherichia coli* DNA polymerase III binds to DNA nonspecifically (*7*). This protein has a ring-shaped tertiary structure lined with cationic residues on its inner surface (*8*).

[†] This work was supported by Grant GM44783 (NIH).

* To whom correspondence should be addressed.

[‡] Department of Biochemistry.

[§] Current address: State University of New York Health Science Center at Syracuse, Department of Biochemistry and Molecular Biology, Syracuse, NY, 13210.

[||] Department of Chemistry.

S0006-2960(98)00743-0 CCC: $15.00
Published on Web 08/15/1998

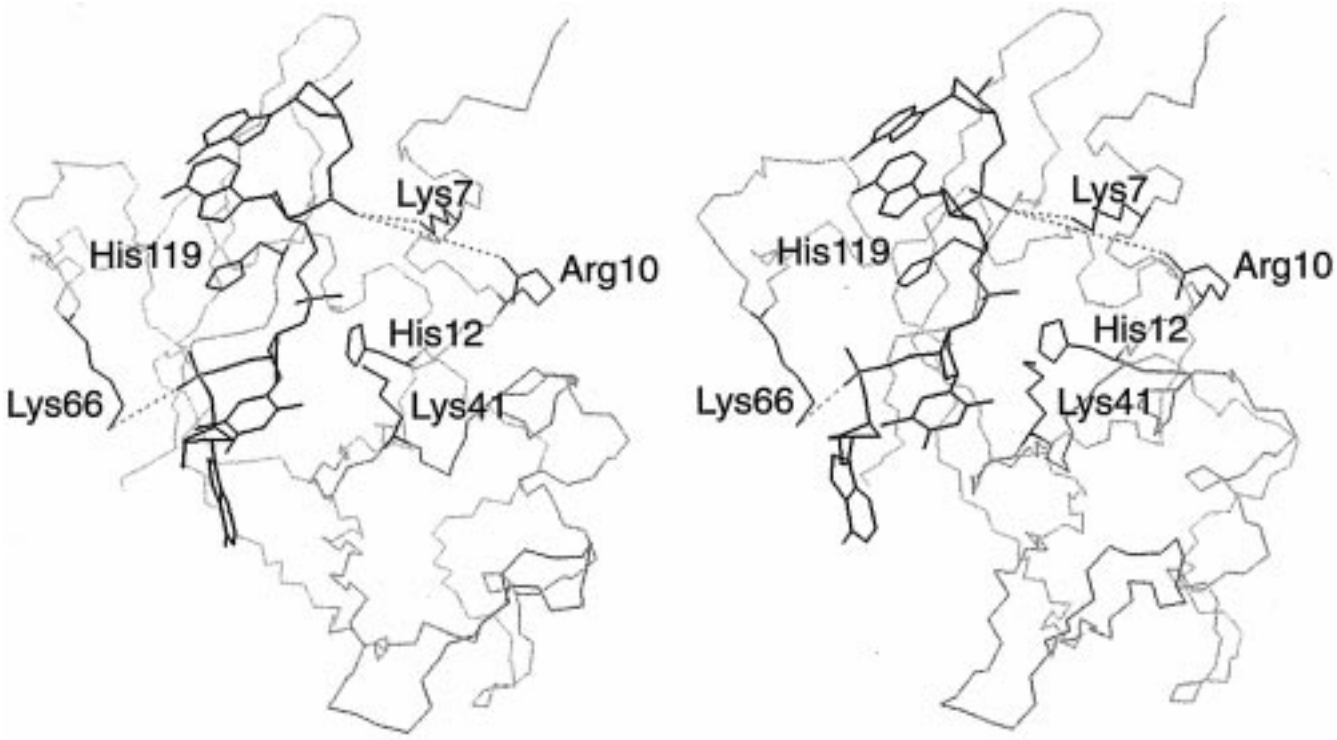

FIGURE 1: Stereoview of the ribonuclease A·d(ATAAG) complex [PDB entry 1rcn (*18*)]. Side chains for Lys7, Arg10, and Lys66 as well as active-site residues His12, His119, and Lys41 are shown. Interactions between residues Lys7, Arg10, and Lys66 and the nearest nonbridging phosphoryl oxygens are indicated by dashed lines.

Complex formation between this subunit and DNA depends primarily on contacts formed between these cationic protein residues and the anionic nucleic acid phosphoryl groups.

Ribonuclease A (RNase A;[1] EC 3.1.27.5) is an endonuclease that catalyzes the cleavage and hydrolysis of single-stranded RNA in two distinct steps (*9*−*11*). Catalysis by RNase A results in the cleavage of the P−$O_{5'}$ bond specifically on the 3′-side of pyrimidine residues (*12*). This enzyme has been the object of landmark work on the folding, stability, and chemistry of proteins; in enzymology; and in molecular evolution (*13*). Because RNase A has been well-characterized, it serves as an excellent model system for studying the details of protein−nucleic acid interactions.

Several studies have suggested that the interactions between RNase A and its RNA substrate extend beyond the scissile bond. RNase A has been shown to destabilize double-stranded DNA by binding to single strands (*14*). Using monovalent cation titration, Record and co-workers have shown that seven ion pairs form between denatured DNA and RNase A (*15*). The structures of crystalline complexes between RNase A and $d(pA)_4$ (*16*), $d(pT)_4$ (*17*), and d(ApTpApApG) (Figure 1) (*18*) also show that there are many interactions between RNase A and polynucleotide ligands. In addition, chemical modification and mutagenesis experiments have divulged the existence of several enzymic subsites (*19*).

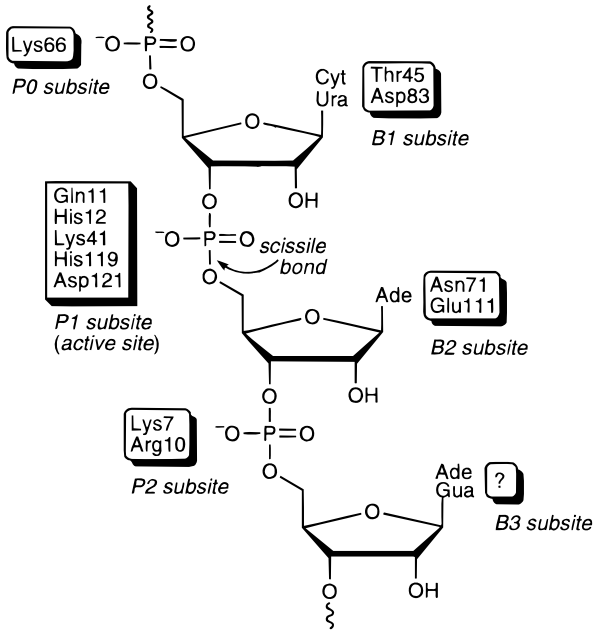

FIGURE 2: Schematic representation of the binding of an RNA fragment to ribonuclease A. The scissile bond is indicated. B and P refer to base and phosphoryl group binding sites, respectively. The twelve indicated residues have been shown by site-directed mutagenesis to make a contribution to substrate binding or turnover (or both) (*13*).

The subsites of RNase A interact with the bases and phosphoryl groups of the bound substrate (Figure 2). There are three known base-binding subsites, B1, B2, and B3. The B1 subsite imparts RNase A with its specificity for cleavage after pyrimidine residues (*16*, *12*). The B2 subsite has a

[1] Abbreviations: *A*, anisotropy; EDN, eosinophil-derived neurotoxin; Fl, fluorescein; HPLC, high-pressure liquid chromatography; *I*, intensity; IPTG, isopropyl-1-thio-β-D-galactopyranoside; K_d, equilibrium dissociation constant; MES, 2-(*N*-morpholino)ethanesulfonic acid; *OD*, optical density; PAGE, polyacrylamide gel electrophoresis; PDB, Brookhaven Protein Data Bank; poly(C), poly(cytidylic acid); pUp, 5′-phosphouridine 3′-phosphate; pU>p, 5′-phosphouridine 2′,3′-cyclic phosphate; RNase A, bovine pancreatic ribonuclease A; SDS, sodium dodecyl sulfate; TB, terrific broth; T_m, midpoint in a thermal denaturation curve; Tris, tris(hydroxymethyl)aminomethane; Up, uridine 3′-phosphate; U>p, uridine 2′,3′-cyclic phosphate.

preference for an adenine base (*20*), and the B3 subsite has a preference for a purine base (*21*, *22*). The important residues in the B1 and B2 subsites have been identified by site-directed mutagenesis experiments (*23*−*26*). The existence of the B3 subsite has been proposed on the basis of kinetic data and chemical modification studies (*21*, *22*, *27*, *28*). The residues comprising the phosphoryl group binding subsites, P0, P1, and P2, have been inferred from similar types of experiments. The phosphoryl group containing the scissile $P-O_{5'}$ resides in the P1 subsite (*29*), which is the enzymic active site. Residues that comprise the P0 and the P2 subsites have been identified by chemical modification, site-directed mutagenesis, and molecular modeling studies. Chemical modification of RNase A by reaction with pyridoxal 5′-phosphate and cyclohexane-1,2-dione implicated Lys7 and Arg10 in the P2 subsite (*30*). Only recently have Lys7 and Arg10 been altered by site-directed mutagenesis (to glutamine residues) to confirm these results (*31*). Lys66 has been proposed as the single residue comprising the P0 subsite, on the basis of molecular modeling and comparison of binding affinities and cleavage rates of substrates of varying length (*29*).

In this study, we characterize in detail the function of the P0 and P2 binding subsites of RNase A. We remove the side chains of Lys7, Arg10, and Lys66 by site-directed mutagenesis of the cDNA encoding the wild-type protein, and produce wild-type RNase A and its K66A, K7A/R10A, and K7A/R10A/K66A variants in *E. coli*. By analyzing catalysis of RNA cleavage, we show that the residues comprising the P0 and P2 subsites interact with the phosphoryl groups adjacent to the scissile bond. In addition, we use fluorescence anisotropy to probe the interaction between a fluorescein-labeled, single-stranded DNA substrate analogue and the wild-type protein and three variants. By comparing the values of the equilibrium dissociation constants (K_d) for the protein·nucleic acid complexes at various salt concentrations, we demonstrate that strong Coulombic interactions exist between Lys7, Arg10, and Lys66 and the bound nucleic acid. In addition, by comparing values of K_d for complex formation in the presence of NaCl to those in the presence of NaF, we find that the anion has only a small effect on binding.

EXPERIMENTAL PROCEDURES

Materials. *E. coli* strain BL21(DE3) (F^- ompT r_B-m_B-) was from Novagen (Madison, WI). *E. coli* strain CJ236 and helper phage M13K07 were from Bio-Rad (Richmond, CA). *E. coli* strain JM109 was from Promega (Madison, WI). All enzymes for the manipulation of recombinant DNA were from either Promega or New England Biolabs (Beverly, MA). Reagents for mutagenesis oligonucleotides were from Applied Biosystems (Foster City, CA), except for acetonitrile, which was from Baxter Healthcare (McGaw Park, IL). Mutagenesis oligonucleotides were synthesized on an Applied Biosystems 392 DNA/RNA synthesizer and purified using Oligo Purification Cartridges from Applied Biosystems (Foster City, CA). DNA was sequenced with a Sequenase 2.0 kit from United States Biochemicals (Cleveland, OH). Poly(cytidylic acid) [poly(C)] was from Midland Certified Reagent (Midland, TX) and was precipitated from aqueous ethanol (70% v/v) before use. Bacto yeast extract, Bacto tryptone, Bacto peptone, and Bacto agar were from Difco (Detroit, MI). Bacterial terrific broth (TB) (*32*) contained (in 1 L) Bacto tryptone (12 g), Bacto yeast extract (24 g), glycerol (4 mL), KH_2PO_4 (2.31 g), and K_2HPO_4 (12.54 g). All media were prepared in distilled, deionized water and autoclaved. Isopropyl-1-thio-β-D-galactopyranoside (IPTG) was from Gold Biotechnology (St. Louis, MO). MES, obtained as the free acid, was from ICN Biomedicals (Aurora, OH). Gel-purified oligonucleotides used for fluorescence anisotropy experiments were obtained from Promega. Sigmacote was from Sigma (St. Louis, MO). All other chemicals and reagents were of commercial grade or better and used without further purification.

General Methods. Ultraviolet and visible absorbance measurements were made with a Cary Model 3 spectrophotometer equipped with a Cary temperature controller from Varian (Sugar Land, TX). RNase A concentrations were determined by assuming that $\epsilon^{0.1\%} = 0.72\ M^{-1}\ cm^{-1}$ at 277.5 nm (*33*). pH was measured with a Beckman pH meter fitted with a Corning electrode, calibrated at room temperature with standard buffers from Fisher (Chicago, IL). Buffer solutions were prepared from the free acid of MES. The Na^+ concentration of the solution was determined using the Henderson−Hasselbalch equation[2] and assuming a pK_a value of 6.15 for MES at 25 °C (*34*).

Site-Directed Mutagenesis. Oligonucleotide-mediated site-directed mutagenesis (*35*) was performed on single-stranded DNA isolated from *E. coli* strain CJ236. To produce the DNA coding for K66A RNase A, the AAG codon for Lys66 in wild-type plasmid pBXR (*26*) was replaced with one coding for alanine (GCT; reverse complement in bold) using the oligonucleotide RR59: TCTGCCCATT**AGC**GCATGCAACATTTT, which also incorporates a translationally silent *Sph*I site (underlined). K7A/R10A RNase A and the triple variant K7A/R10A/K66A RNase A were created by replacing the AAG codon for Lys7 and the CGG codon for Arg10 with ones coding for alanine (GCT; GCG; reverse complements in bold) in the wild-type or K66A RNase A cDNA using the oligonucleotide BT1: TCCATGTGCTG**CGC**CTCAAA**CGC**AGCTGCTGCAGTT, which also incorporates a translationally silent *Pvu*II site (underlined). Mutagenesis reaction mixtures were transformed into competent JM109 cells, and the isolated plasmid DNA of the transformants was analyzed by sequencing.

Protein Production and Purification. A glycerol freeze of *E. coli* strain BL21(DE3) harboring wild-type or mutant plasmids was prepared from a mid-log phase culture grown in LB medium containing ampicillin (400 μg/mL). Wild-type and variant proteins were produced and purified essentially as described elsewhere (*36*, *37*), except on a larger scale. To produce protein, glycerol freezes were streaked onto LB-agar plates containing ampicillin (100 μg/mL). A single colony was then used to inoculate a starter culture (20 mL) of LB medium containing ampicillin (400 μg/mL). Upon reaching mid-log phase ($OD = 1.0$ at 600 nm), this culture was used to inoculate a larger starter culture (500 mL) of TB medium containing ampicillin (400 μg/mL). Both inoculated cultures were shaken (250 rpm) at 37 °C. This starter culture was used to inoculate a 12 L fermenter flask of TB containing ampicillin (400 μg/mL). cDNA expression

[2] Using the Henderson−Hasselbalch equation, 0.10 M MES−NaOH buffer (pH 6.0) has $[Na^+] = 0.042$ M.

was induced by the addition of IPTG (to 0.5 mM) at the late-log phase ($OD = 2.0$ at 600 nm). Cells were harvested by centrifugation 2−4 h after induction and resuspended in 1/100 volume of cell lysis buffer, which was 20 mM Tris−HCl buffer (pH 8.0) containing EDTA (10 mM). Cells were broken by passing through a French pressure cell three times. Proteins were solubilized from inclusion bodies, denatured and reduced, folded/oxidized in vitro, concentrated by ultrafiltration, and purified by loading on a Pharmacia FPLC HiLoad 26/60 Superdex 75 gel filtration column (Piscataway, NJ) that had been equilibrated with 50 mM sodium acetate buffer (pH 5.0) containing NaCl (0.10 M) and NaN_3 (0.02% w/v). Fractions corresponding to monomeric protein, which eluted at 192−220 mL, were pooled and loaded onto an FPLC mono-S cation exchange column (15 cm × 1.8 cm^2) that had been equilibrated with 50 mM sodium acetate buffer (pH 5.0). RNase A was eluted with a linear gradient (50 mL + 50 mL) of NaCl (0.1−0.3 M) in sodium acetate buffer (pH 5.0). Protein fractions were pooled and characterized. SDS−polyacrylamide gel electrophoresis, zymogram electrophoresis (*38*−*40*), and A_{280}/A_{260} ratios greater than 1.8 (*41*) indicated that the proteins were >99% pure. N-terminal sequence analysis of purified protein was determined by automated Edman degradation at the Protein and Nucleic Acid Chemistry Laboratory (Washington University, St. Louis, MO).

Thermal Denaturation. The stabilities of the wild-type and variant enzymes were determined by thermal denaturation studies. As RNase A is denatured, its six tyrosine residues become exposed to solvent and its molar absorptivity at 287 nm decreases significantly (*42*). By monitoring the change in absorbance at 287 nm with temperature, the thermal stability of RNase A can be assessed (*25*, *43*, *44*). Solutions of protein (70−210 μM) were prepared in 0.030 M sodium acetate buffer (pH 6.0) containing 0.10 M NaCl. The absorbance at 287 nm was recorded as the temperature was increased from 25 to 90 °C in 1 °C increments, with a 5 min equilibration at each temperature. Similarly, the absorbance at 287 nm was recorded as the temperature was decreased from 90 to 25 °C. The data were fit to a two-state model for denaturation, and T_m (the midpoint in the thermal denaturation curve) was calculated using the program SIGMA PLOT 4.16 (Jandel Scientific; San Rafael, CA).

Steady-State Kinetic Analysis. Spectrophotometric assays were used to determine the steady-state kinetic parameters for the cleavage of poly(C). The cleavage of poly(C) was monitored by following a change in ultraviolet hyperchromicity. The $\Delta\epsilon$ for this reaction, calculated from the difference in molar absorptivity of the polymeric substrate and the mononucleotide cyclic phosphate product, is 2380 M^{-1} cm^{-1} at 250 nm (*25*). Assays were performed at 25 °C in 0.10 M MES−NaOH buffer (pH 6.0) containing NaCl (0.10 M), poly(C) (10 μM−1.6 mM), and enzyme (21 pM−3.3 nM). The values of k_{cat}, K_m, and k_{cat}/K_m were determined from initial velocity data with the program HYPERO (*45*).

Thermodynamic Cycles. The degree of interaction between altered residues in RNase A can be determined by examining thermodynamic cycles calculated from steady-state kinetic parameters for the cleavage of poly(C). The change in the contribution of free energy ($\Delta\Delta G$) to catalysis due to a particular protein variation was calculated from eq 1, where f is the ratio of a particular kinetic or thermodynamic parameter for the two enzymes being compared (*26*):

$$\Delta\Delta G = RT \ln f \tag{1}$$

For example, the contribution of free energy to binding of the rate-limiting transition state (*46*, *47*) by the side chain of Lys66 was calculated from eq 2:

$$\Delta\Delta G_{wt\rightarrow K66A} = RT \ln\left[\frac{(k_{cat}/K_m)_{wt}}{(k_{cat}/K_m)_{K66A}}\right] \tag{2}$$

The contribution of free energy to catalysis from the interaction between the residues under investigation was calculated from eq 3 as described previously (*48*−*51*).

$$\Delta\Delta G_{int} = \Delta\Delta G_{wt\rightarrow K7A/R10A/K66A} - \Delta\Delta G_{wt\rightarrow K7A/R10A} - \Delta\Delta G_{wt\rightarrow K66A} \tag{3}$$

Fluorescence Anisotropy. Fluorescence anisotropy assays are based on the increase in the rotational correlation time of a fluorophore upon binding of a fluorophore-labeled oligonucleotide to a protein (*52*, *53*). The protein·oligonucleotide complex, due to its increased molecular volume, tumbles more slowly than does the free, labeled oligonucleotide. The ensuing reduction in the rotational correlation time of the fluorophore causes an increase in anisotropy, which allows binding to be monitored (*54*). As shown in eq 4, anisotropy (A) is defined as the ratio of the difference

$$A = 10^3 \text{ mA} = \frac{I_{||} - I_{\perp}}{I_{||} + 2I_{\perp}} \tag{4}$$

between the vertical (||) and horizontal ($\perp$) emission components with respect to the total intensity (I) when vertically polarized excitation is used.

The oligonucleotide used in the fluorescence anisotropy assays was fluorescein∼d(AUAA) [Fl∼d(AUAA); Figure 3]. Fluorescein, incorporated via a phosphoramidite derivative during the final coupling step of DNA synthesis, was attached to the 5′ end of the oligonucleotide by a six-carbon spacer to the terminal 5′-OH. Following synthesis, the oligonucleotide was gel-purified, desalted, and analyzed for homogeneity by reversed-phased HPLC and capillary electrophoresis (D. Leland, personal communication). The concentration of oligonucleotide was determined by summing the ϵ for fluorescein and the four bases to yield ϵ = 66250 M^{-1} cm^{-1} at 260 nm (*55*).

Fluorescence anisotropy was measured at room temperature (23 ± 2 °C) on a Beacon Fluorescence Polarization System from PanVera (Madison, WI) with excitation at 488 nm and emission at 520 nm. Protein (0.2−2 mM) that had been dialyzed exhaustively against water and lyophilized was dissolved in 1.8 mL of 0.020 or 0.10 M MES−NaOH buffer (pH 6.0) containing NaCl (0.010−0.10 M). Fluorescein-labeled oligonucleotide, diluted in the same buffer, was added to half of the protein solution to a final concentration of 2.0 nM. The sample volume was then adjusted to 1.0 mL by the addition of buffer. Similarly, a blank tube was prepared by diluting the remaining half of the protein solution with buffer to 1.0 mL. Sigmacote was used to prepare silinized glass tubes, which were used for all anisotropy

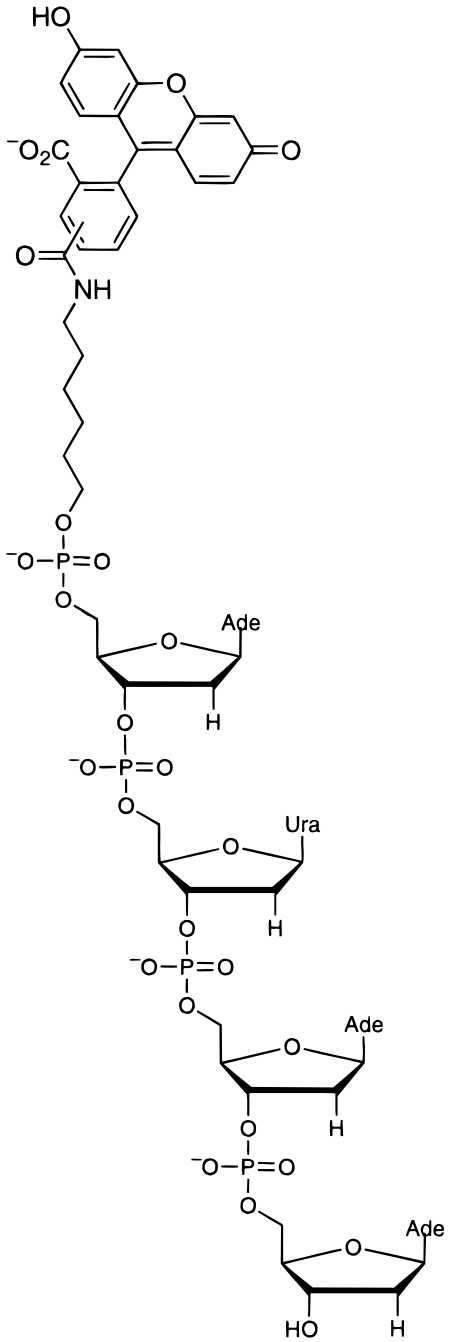

FIGURE 3: Fluorescein-labeled oligonucleotide [Fl∼d(AUAA)] used for fluorescence anisotropy experiments. The design of this oligonucleotide was based on the oligonucleotide in a crystalline ribonuclease A·d(ATAAG) complex (*18*).

measurements to reduce the adherence of protein to the glass. Measurements (6−8) were made at this protein concentration before diluting the sample and the blank. Dilution of the sample entailed removing an aliquot (0.25 mL) and replacing it with an aliquot (0.25 mL) of a 2.0 nM oligonucleotide solution. The blank was diluted similarly, except that buffer, rather than oligonucleotide solution, was used. Reading of the blank, then the sample, followed by the dilution step, was repeated up to thirty times for each binding experiment. At the end of each experiment, the RNase A concentration in an aliquot of sample tubes 1, 4, and 7 was determined. The remaining protein concentrations were calculated by assuming constant dilutions of three-fourths for each concentration. The equilibrium dissociation constants were determined by fitting the average anisotropy value at each protein concentration to eq 5, which describes binding to a single specific site (*56*). Binding parameters were determined by a nonlinear least-squares analysis, which was weighted by the inverse of the standard deviation of each reading, using the program DELTA GRAPH 4.0 (DeltaPoint; Monterey, CA).

Table 1: Steady-State Kinetic Parameters for the Cleavage of Poly(C) by Wild-Type Ribonuclease A, and the K66A, K7A/R10A, and K7A/R10A/K66A Variants[a]

RNase A (T_m; °C)[b]	k_{cat} (s^{-1})	K_m (mM)	k_{cat}/K_m ($10^6\ M^{-1}\ s^{-1}$)
wild-type (62)	507 ± 15	0.089 ± 0.009	5.7 ± 0.5
K66A (60)	365 ± 7	0.202 ± 0.014	1.8 ± 0.1
K7A/R10A (58)	22.7 ± 1.0	0.222 ± 0.027	0.10 ± 0.01
K7A/R10A/K66A (57)	16.7 ± 0.7	0.907 ± 0.077	0.018 ± 0.002

[a] Data were obtained at 25 °C in 0.10 M MES−NaOH buffer (pH 6.0) containing NaCl (0.10 M). [b] Values of T_m are reported ± 2 °C.

$$A = \frac{\Delta A[\text{RNaseA}]}{K_d + [\text{RNaseA}]} + A_{min} \quad (5)$$

In eq 5, A is the average of the measured fluorescence anisotropy values, ΔA ($A_{max} - A_{min}$) is the total change in anisotropy, and A_{min} is the anisotropy value of the unbound oligonucleotide. [RNase A] is protein concentration, and K_d is the equilibrium dissociation constant.

RESULTS

Protein Production and Purification. A recombinant DNA system developed in our laboratory was used to direct the expression of wild-type, K66A, K7A/R10A, and K7A/R10A/K66A RNase A (*37*). This system utilizes the *E. coli* T7 RNA polymerase expression system, and after several purification steps yields approximately 50 mg of pure wild-type protein/L of culture. Following the expression of appropriately mutated cDNA in *E. coli* strain BL21(DE3), similar protein yields were obtained of pure K66A RNase A, K7A/R10A RNase A, and K7A/R10A/K66A RNase A. K66A RNase A migrated similarly to the wild-type protein during SDS−PAGE. In contrast, both the double and triple variants migrated more slowly than did the wild-type protein (data not shown). To ascertain that the pelB leader sequence had been cleaved properly from the N terminal of the protein, the double variant K7A/R10A RNase A was subjected to N-terminal sequence analysis. The sequence of the eight N-terminal amino acid residues indicated that proper proteolytic processing had occurred. Because both the double and the triple variant migrated similarly, we assume that the slower migration during SDS−PAGE in comparison to wild-type protein is a result of removing the positive charges at residues 7 and 10. This result is consistent with the slower migration during SDS−PAGE seen by Cuchillo and co-workers for R7Q/R10Q RNase A (*31*).

Steady-State Kinetic Parameters. Steady-state kinetic parameters for the cleavage of poly(C) are listed in Table 1. Also listed in this table are the values of T_m determined for the three variant proteins. The values of T_m, which are all within 6 °C of the T_m for the wild-type protein, indicate that the kinetic parameters determined at 25 °C are indeed those

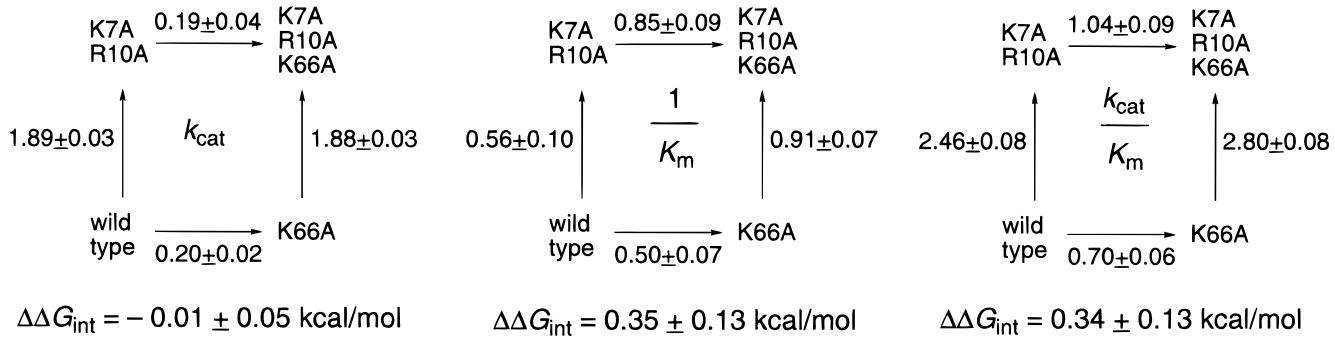

FIGURE 4: Thermodynamic cycles for the cleavage of poly(C) by ribonuclease A upon replacing Lys7 and Arg10, Lys66, or all three residues with alanine. The cycles are drawn for the steady-state kinetic parameters k_{cat} (left), $1/K_m$ (middle), and k_{cat}/K_m (right) with values (in kcal/mol) derived from equations analogous to eq 2. The values for the interaction free energies, $\Delta\Delta G_{int}$, were determined using eq 3.

of native, rather than denatured, proteins. In addition, we have determined the crystalline structure of K7A/R10A/K66A RNase A, both with and without bound uridine 3′-phosphate [PDB entries 3rsk and 4rsk, respectively (*57*)]. The structure of K7A/R10A/K66A RNase A is essentially identical to that of the wild-type protein. Hence, any changes in function from replacing Lys7, Arg10, and Lys66 are not due to changes in structure.

Replacing Lys66, Lys7, and Arg10, or all three of these residues with alanine has an effect on the values of both K_m and k_{cat} for the cleavage of poly(C). The k_{cat} for poly(C) cleavage by K66A RNase A is similar to that of the wild-type protein, and the K_m is increased by 2−3-fold. The k_{cat} for poly(C) cleavage by K7A/R10A RNase A is reduced by 20-fold, and the K_m is increased by 2−3-fold as compared to the values for cleavage by the wild-type enzyme. The K7A/R10A/K66A variant showed a 20-fold reduction in k_{cat} for poly(C) cleavage and a 10-fold increase in K_m. The values of k_{cat}/K_m for catalysis of poly(C) cleavage by the K66A, K7A/R10A, and K7A/R10A/K66A variants were observed to be 3-fold, 60-fold, and 300-fold lower, respectively, than that of wild-type RNase A.

Thermodynamic Cycles for the Cleavage of Poly(C). Thermodynamic cycles that relate the free energies corresponding to k_{cat}, K_m, and k_{cat}/K_m for the cleavage of poly(C) by wild-type RNase A and the K66A, K7A/R10A, and K7A/R10A/K66A variants are shown in Figure 4. The effect of a substitution on the free energy relating to k_{cat}, K_m, or k_{cat}/K_m (which reports on the binding of the rate-limiting transition state) can be determined from the k_{cat}, $1/K_m$, and k_{cat}/K_m thermodynamic cycles, respectively. The P0 subsite, which consists of Lys66, contributes 0.20 kcal/mol to the value of k_{cat}, 0.50 kcal/mol to the value of K_m, and 0.70 kcal/mol to the binding of the rate-limiting transition state. The P2 subsite, which consists of Lys7 and Arg10, makes a similar contribution to the free energy corresponding to K_m but a larger contribution to the value of k_{cat} and the binding of the rate-limiting transition state than does the P0 subsite. The contribution of the P2 subsite is 1.89 kcal/mol to the value of k_{cat}, 0.56 kcal/mol to the value of K_m, and 2.46 kcal/mol to transition-state binding. The P0 and P2 subsites interact during catalysis of poly(C) cleavage. The contributions to the free energy of the K_m value and the binding of the transition state due to this interaction are 0.35 and 0.34 kcal/mol, respectively.

DNA Binding to Wild-Type and Three RNase A Variants. RNase A binds to single-stranded DNA (*58*) but cannot cleave this biopolymer. Therefore, single-stranded DNA is an excellent analogue of RNA with which to investigate the binding (without turnover) of a substrate to RNase A. The three-dimensional structure of the crystalline complex of d(ATAAG) with wild-type RNase A [PDB entry 1rcn (*18*)] shows that this oligomer binds to both the active site and the distal subsites of RNase A. Thus this or a similar oligomer can be used to reveal meaningful aspects of substrate binding to RNase A.

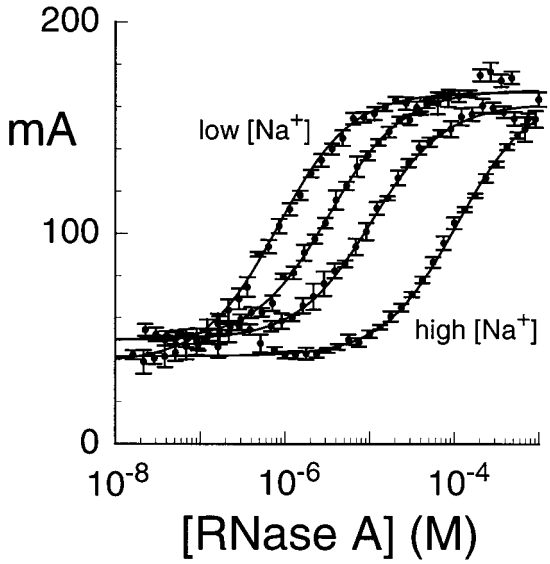

FIGURE 5: Raw data for binding of fluorescein∼d(AUAA) to wild-type ribonuclease A at four [Na^+]. Binding was measured by fluorescence anisotropy at 23 ± 2 °C in 0.020 M MES−NaOH buffer containing fluorescein∼d(AUAA) (2.0 nM) and NaCl (0.010, 0.025, or 0.050 M) or in 0.10 M MES−NaOH buffer (pH 6.0) containing fluorescein∼d(AUAA) (2.0 nM) and NaCl (0.10 M). Each data point is the average of 6−8 measurements, with the standard deviation for each point indicated by the bars. The curves are best fits to eq 5.

The results of fluorescence anisotropy assays with Fl∼d(AUAA) binding to the wild-type protein demonstrated that this technique was suitable for assaying complex formation. The affinity of Fl∼d(AUAA) to wild-type RNase A in four aqueous solutions that differ in [Na^+] is shown in Figure 5. As the [Na^+] increased, the affinity of this oligomer for RNase A decreased. The difference in anisotropy values between free and bound oligomer, which was approximately ΔA = 120 mA units, was constant in all of the binding experiments with the wild-type protein. In addition, this value was similar to the change in anisotropy seen when

Table 2: Effect of NaCl on the Values of K_d (μM) for Binding of Fluorescein∼d(AUAA) to Wild-Type Ribonuclease A and the K66A, K7A/R10A, and K7A/R10A/K66A Variants[a]

	[Na^+] (M)			
RNase A	0.018[b]	0.033[b]	0.059[b]	0.142[c]
wild-type	0.82	3.1	11	88
K66A	11	33	110	400
K7A/R10A	35	100	260	640
K7A/R10A/K66A	220	520	440[d]	1600

[a] All data were were collected on a Beacon Fluorescence Polarization System (Panvera; Madison, WI) at 23 ± 2 °C. The error on the curve fitting, determined using the program BIOEQS (*60*−*62*), was typically <5%. The errors determined from duplicate experiments were closer to 15%. We therefore assume the real error on each of these points to be ≤15% and do not report the errors determined from curve fitting, which are presumably underestimates. [b] Determined in 0.020 M MES−NaOH buffer (pH 6.0) containing fluorescein∼d(AUAA) (2.0 nM) and NaCl (to the indicated [Na^+]). [c] Determined in 0.10 M MES−NaOH buffer (pH 6.0) containing fluorescein∼d(AUAA) (2.0 nM) and NaCl (0.10 M). [d] Determined in 0.10 M MES−NaOH buffer (pH 6.0) containing fluorescein∼d(AUAA) (2.0 nM) and NaCl (0.040 M) ([Na^+] = 0.049 M).

Fl∼d(UAA) binds to wild-type RNase A (*59*). The total fluorescence intensity decreased at the beginning of the titrations, but remained constant at the end of the titrations, when protein concentrations were low. This change in total intensity, which was observed in all binding experiments, could have resulted from light scattering at high protein concentrations.

Binding of Fl∼d(AUAA) to K66A RNase A, K7A/R10A RNase A, and K7A/R10A/K66A RNase A at varying salt conditions was also examined by using fluorescence anisotropy. It was not possible to saturate the oligomer with K7A/R10A RNase A or K7A/R10A/K66A RNase A at high salt concentrations, due to weak binding. The solubility of protein precluded a direct determination of anisotropy values for completely bound oligomer to these variants under these conditions. To fit the data for these titrations, we used the $\Delta A = 120$ mA value that was determined for the binding of this oligomer to the wild-type protein. The dissociation constants for these binding experiments are listed in Table 2.

As listed in Table 2, Fl∼d(AUAA) bound more tightly to wild-type protein than to any of the variants at solution conditions equivalent to those used for the kinetic experiments [that is, 0.10 M MES−NaOH (pH 6.0) containing NaCl (0.10 M)]. The K_d values increased in the following order: wild-type RNase A < K66A RNase A < K7A/R10A RNase A < K7A/R10A/K66A RNase A. At lower [Na^+], the same trend was seen, but the differences in K_d values were larger. These trends are more apparent when plotted on a logarithmic scale, as shown in Figure 6. It is apparent from the slopes of the lines in Figure 6 that oligomer binding to the wild-type protein had the highest salt concentration dependence, and binding to K7A/R10A/K66A RNase A had the lowest salt concentration dependence.

Effect of NaF on ssDNA Binding. The effect of anions on the binding of RNase A to Fl∼d(AUAA) was examined using fluorescence anisotropy assays. Values of K_d for the complex of wild-type protein with Fl∼d(AUAA) were determined at four different NaF concentrations, in 0.020 or 0.10 M MES−NaOH buffer (pH 6.0). These K_d values are listed in Table 3 and plotted versus cation concentration on a log−log scale in Figure 7. As shown in Figure 7, the binding of wild-type RNase A to Fl∼d(AUAA) binding was only slightly tighter in the presence of NaF than in the presence of NaCl, at all but the lowest concentration examined. In addition, the salt concentration dependence of binding was slightly weaker in the presence of NaF than in the presence of NaCl.

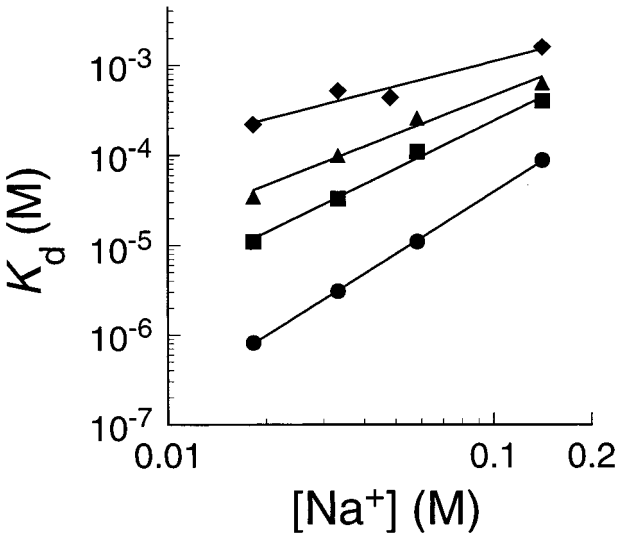

FIGURE 6: Transformed data for binding of fluorescein∼d(AUAA) to wild-type ribonuclease A (●), and the K66A (■), K7A/R10A (▲), and K7A/R10A/K66A (◆) variants at four [Na^+]. Binding was measured by fluorescence anisotropy at 23 ± 2 °C in 0.020 M MES−NaOH buffer (pH 6.0) containing fluorescein∼d(AUAA) (2.0 nM) and NaCl [0.010, 0.025, or 0.050 M (0.040 M for K7A/R10A/K66A ribonuclease A)] or in 0.10 M MES−NaOH buffer (pH 6.0) containing fluorescein∼d(AUAA) (2.0 nM) and NaCl (0.10 M). The slopes of the lines are 2.3 ± 0.1 (wild-type), 1.8 ± 0.1 (K66A), 1.4 ± 0.1 (K7A/R10A), and 0.9 ± 0.2 (K7A/R10A/K66A).

Table 3: Comparison of the Effect of NaCl and NaF on the Values of K_d (μM) for the Binding of Fluorescein∼d(AUAA) to Wild-Type Ribonuclease A[a]

	[Na^+] (M)			
salt	0.018[b]	0.033[b]	0.059[b]	0.142[c]
NaCl	0.82	3.1	11	88
NaF	1.1	2.4	7.1	61

[a] All data were were collected on a Beacon Fluorescence Polarization System at 23 ± 3 °C. [b] Determined in 0.020 M MES−NaOH buffer (pH 6.0) containing fluorescein∼d(AUAA) (2.0 nM) and NaCl (to the indicated [Na^+]). [c] Determined in 0.10 M MES−NaOH buffer (pH 6.0) containing fluorescein∼d(AUAA) (2.0 nM) and NaCl (0.10 M).

DISCUSSION

In native RNase A, the residues His12, His119, and Lys41 are in close proximity to each other (*63*). These residues, though they are the primary residues directly involved in catalysis of RNA cleavage, do not act alone. Several other residues interact with the RNA substrate, thereby playing important auxiliary roles in catalysis. In this work, we characterize in detail the function of three such residues: Lys7, Arg10, and Lys66.

RNase A appears to have evolved to catalyze the cleavage of RNA rather than its hydrolysis (*10*, *11*). Here, we used two tools to characterize the interactions involved in nucleic

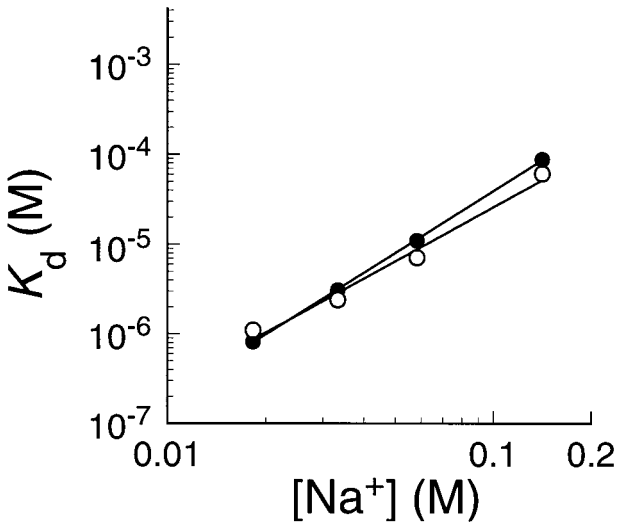

FIGURE 7: Transformed data for binding of fluorescein∼d(AUAA) to wild-type ribonuclease A in the presence of different anions. Binding was assayed by fluorescence anisotropy in the presence of NaCl (●) and NaF (○). Binding was measured at 23 ± 2 °C in 0.020 M MES−NaOH buffer containing fluorescein∼d(AUAA) (2.0 nM) and NaCl or NaF (0.010, 0.025, or 0.050 M) or in 0.10 M MES−NaOH buffer (pH 6.0) containing fluorescein∼d(AUAA) (2.0 nM) and NaCl or NaF (0.10 M). The slopes of the lines are 2.3 ± 0.1 (NaCl) and 2.0 ± 0.2 (NaF).

acid recognition and complex formation by RNase A, interactions that necessarily precede the cleavage of RNA. First, we investigated protein−nucleic acid interactions during catalysis of RNA cleavage by wild-type RNase A and three variants using spectrophotometric assays. Second, we used fluorescence anisotropy experiments to investigate binding (without turnover) of a substrate analogue to RNase A. Fluorescence anisotropy is a useful method for studying protein−nucleic acid interactions in solution, where the effect of changing conditions such as pH, temperature, or salt concentration can be ascertained readily (*52*). Previous studies employing this technique have investigated the binding of a protein to a fluorescein-labeled, double-stranded DNA of >20 base pairs (*52, 54, 64, 65*). We report the use of this technique to investigate the binding of a protein to a single-stranded DNA oligonucleotide of only 4 bases.

Lys66 Comprises the RNase A P0 Subsite. The hypothesis that Lys66 comprises the P0 subsite of RNase A had been based on the results of several studies, including a comparison of the binding affinity of 5′-phosphouridine 3′-phosphate (pUp) versus uridine 3′-phosphate (Up) to RNase A (*66*), a comparison of the rates of cleavage of 5′-phosphouridine 2′,3′-cyclic phosphate (pU>p) versus uridine 2′,3′-cyclic phosphate (U>p) (*67*), an X-ray diffraction analysis (*68*), molecular modeling (*69*), and its evolutionary conservation among 40 of the 41 known pancreatic ribonuclease sequences (*70*, *71*). This residue had never been subjected to chemical modification or been replaced with another amino acid (*13*).

Lys66 is removed from the active site of RNase A, with N_ζ of Lys66 being 7.3 Å from the nearest active-site histidine residue, His119 [PDB entry 7rsa (*72*)]. In contrast, N_ζ of Lys66 is only 5.3 Å from the nearest phosphoryl group oxygen atom of a bound oligonucleotide (*18*), that which is 5′ to the scissile phosphodiester bond (Figure 1). Thus, it is no surprise that removing the Lys66 side chain has a less profound effect on the value of k_{cat} for the cleavage of a polymeric substrate than on the value of K_m. The observed >2-fold increase in K_m for poly(C) cleavage suggests that the side chain of Lys66 does interact with this polymeric substrate during catalysis. Binding of Fl∼d(AUAA) to K66A RNase A under similar solution conditions [0.10 M MES−NaOH (pH 6.0) containing NaCl (0.10 M)] yields a similar result. The value of K_d for the binding of Fl∼d(AUAA) to RNase A is increased by 4.5-fold upon the removal of the Lys66 side chain. Thus, data from both kinetic and thermodynamic approaches indicate that Lys66 interacts with the substrate phosphoryl group that is 5′ to the scissile phosphodiester bond.

Lys66 is Not Required for Catalysis by RNase A. The conservation of a lysine residue at position 66 of RNase A implicates it as being important in catalysis. Beintema hypothesized that a cationic amino acid residue at either position 66 or position 122 is required for catalytic activity by members of the ribonuclease superfamily (*73*). He compared the more active members of the ribonuclease superfamily, such as the mammalian pancreatic and other secretory ribonucleases, to less active members of this family, such as human and bovine angiogenin and eosinophil-derived neurotoxin (EDN), and found that the less active members of this superfamily have deletions or insertions at position 66. Where a basic residue was absent at position 66 in the more active family members, a cationic residue was present at position 122. Position 122 in RNase A is a serine residue. So by this hypothesis, position 66 must be a cationic residue for RNase A to maintain high catalytic activity. The removal of the cationic side chain of Lys66 in RNase A results in only a small decrease in enzymatic activity; the value of k_{cat}/K_m is reduced by ∼3-fold for the cleavage of poly(C). In contrast, EDN cleaves poly(C) 2×10^3-fold slower than does RNase A (*74*). Apparently, a cationic residue at position 66 or position 122 is not necessary for high catalytic activity.

Roles of Lys7 and Arg10 in Catalysis. Similarly to Lys66, the role of Lys7 and Arg10 was proposed originally on the basis of X-ray diffraction analyses and molecular modeling. But unlike with Lys66, the role of these residues has been confirmed by chemical modification and mutagenesis experiments, which showed more directly the presence of these residues in the P2 subsite. The characterization of the single variants K7Q RNase A and R10Q RNase A by Cuchillo and co-workers suggests that the side chains of Lys7 and Arg10 must both be replaced to see a significant effect on catalysis by RNase A (*31*). N_ζ of Lys7 is 3.1 Å from the nearest phosphoryl oxygen of a bound nucleic acid, and the nearest guanido N of Arg10 is 7.7 Å from this same oxygen (Figure 1). Considering only proximity, one might surmise that Lys7 plays a more prominent role in interacting with the substrate, with Arg10 playing merely a compensatory role in its absence. To characterize the entire P2 subsite, we created an RNase A variant in which both Lys7 and Arg10 were changed to alanine residues.

The removal of the Lys7 and Arg10 side chains affects profoundly both the values of K_m and k_{cat} for cleavage of the polymeric substrate poly(C) and the value of K_d for binding of Fl∼d(AUAA) under similar conditions. The K_m is increased by 2.5-fold and the k_{cat} is decreased by 20-fold relative to cleavage by the wild-type enzyme. The k_{cat}/K_m is decreased by 60-fold. The K_d is increased 7-fold. Cuchillo

and co-workers observed similar effects on the kinetic parameters for poly(C) cleavage upon replacing Lys7 and Arg10 with glutamine residues (*31*). They observed a 3.6-fold increase in K_m, a 17-fold decrease in k_{cat}, and a 60-fold decrease in k_{cat}/K_m. Glutamine residues do not bear a charge, but they do have the capacity to donate hydrogen bonds. Although the side chain of a glutamine residue is shorter than that of either a lysine or an arginine residue, our molecular modeling indicates that glutamine residues at positions 7 and 10 can interact with a phosphoryl group of a bound RNA substrate. The similarity in the kinetic parameters for the glutamine and alanine variants at positions 7 and 10 in RNase A suggests that Coulombic interactions, and not hydrogen bonds, are the critical interactions formed between the P2 subsite and the phosphoryl group 3′ to the scissile phosphodiester bond on the RNA substrate.

Synergy between the P0 and P2 Subsites. Small interaction free energies (≤1 kcal/mol) between protein residues that are not in direct contact is a common feature in proteins (*75*). In RNase A, the N_ζ atom of Lys66 is 16 Å from the N_ζ atom of Lys7 and 19 Å from either guanido N atom of Arg10 (*72*). From this distance, the P0 subsite cannot interact directly with the P2 subsite. From the kinetic parameters for the cleavage of poly(C) by wild-type RNase A and the three variants, we find that the free energies contributed by each of these subsites are additive in terms of k_{cat} ($\Delta\Delta G_{int} = -0.01$ kcal/mol) but are nonadditive in terms of K_m ($\Delta\Delta G_{int} = 0.34$ kcal/mol) and k_{cat}/K_m ($\Delta\Delta G_{int} = 0.35$ kcal/mol) (Figure 4). Analyses of multiple pairs of mutations in different proteins have, however, shown that small interaction free energies appear to be nonrandom and, therefore, significant (*75*). Although small, the interaction free energies we observe may report on a synergistic loss of entropy upon binding of both the substrate and the transition state.

Effect of NaCl on Fl∼d(AUAA) Binding to Wild-Type RNase A and Three Variants. The effect of NaCl concentration on the binding affinity of ssDNA for RNase A was first demonstrated by Jensen and von Hippel (*14*). Using a boundary sedimentation velocity technique, they found that single-stranded calf thymus DNA, which is heterogeneous and binds several protein molecules per strand, has a strong salt concentration dependence for binding to RNase A. This dependence is a result of the polyanionic nature of DNA, which accumulates a high local concentration of mobile counterions (e.g., Na^+) and a low local concentration of mobile co-ions (e.g., Cl^-) (*76*). Accumulated cations are released from the polymeric DNA strand upon complex formation. Concomitantly, anions are released from the protein. The accompanying increase in entropy is a driving force for binding (*15*). From the slope of a log K_d versus log [Na^+] plot, one can determine the number of ion pairs formed between the DNA ligand and the protein, and also the number of cations and anions released upon binding. Record and co-workers analyzed the data of Jensen and von Hippel in this manner, finding that seven ion pairs are formed between polymeric ssDNA and RNase A (*15*).

In our binding experiments, we used a small (4-base), single-stranded oligonucleotide. We based the design of our oligonucleotide, Fl∼d(AUAA), on the high-resolution crystalline structure of the complex between d(ATAAG) and RNase A (Figure 1). Our oligonucleotide spans both the active site and the distal subsites of RNase A and forms a protein·ligand complex with a stoichiometry of 1. The small size of this oligonucleotide makes a quantitative analysis of our data difficult. Short oligonucleotides, such as the tetramer used here, are oligoelectrolytes and differ strikingly from polyelectrolytes in their interactions with salt ions (*77*). A nucleic acid strand can be considered to be a polyelectrolyte if there are more than 18 DNA monomer units (i.e., 36 phosphoryl groups) (*78*); our oligomer falls well short of this value. Thus, the small size of our oligonucleotide makes it impossible to use polyelectrolyte theory to interpret the slopes from log−log plots in terms of the number of ion pairs formed upon binding. Nevertheless, the conclusion from a qualitative analysis of our binding data is consistent with that from of our kinetic experiments: Coulombic forces mediate the interactions between the P0 and P2 subsites and a molecule of RNA.

In agreement with the results of Jensen and von Hippel (*14*), we find that the affinity of ssDNA for wild-type RNase A is influenced dramatically by the concentration of NaCl. The values of K_d and cation concentrations from Table 2 are plotted in Figure 6. The value of $\partial \log K_d/\partial \log [Na^+]$ for the binding of Fl∼d(AUAA) to wild-type RNase A is 2.3 ± 0.1. For the reasons described above, we cannot quantitate this value in terms of cations released from the DNA or number of ion pairs formed in the complex. Still, this value can be compared to those for the binding of the same oligonucleotide to the three variant proteins. Changing RNase A residues that are involved in Coulombic interactions with the substrate is expected to result in binding affinities with a weaker dependence on salt concentration. We find such an effect. From the plots in Figure 6, the values of $\partial \log K_d/\partial \log [Na^+]$ are 1.8 ± 0.1 for Fl∼d(AUAA) binding to K66A RNase A, 1.4 ± 0.1 for Fl∼d(AUAA) binding to K7A/R10A RNase A, and 0.9 ± 0.2 for Fl∼d(AUAA) binding to K7A/R10A/K66A RNase A. From these values, we conclude that the P0 and P2 subsites engage in Coulombic interactions with the phosphoryl groups of a bound single-stranded nucleic acid.

Comparison of the K_d Values for Fl∼d(AUAA) Binding to Wild-Type RNase A in Buffer Containing NaF versus NaCl. Anions can interact with proteins. Studies with several nucleic acid-binding proteins (*79*−*83*) have shown that values of K_d for complex formation in buffers differing only in the anion tend to follow the Hofmeister series (*84*), which ranks anions in the following order: $F^- < SO_4^{2-} < HPO_4^{2-} < CH_3CO_2^- < Cl^- < Br^- < NO_3^- < I^- < CCl_3CO_2^- < ClO_4^- < SCN^-$. This order is similar to the ability of anions to interact with proteins, with fluoride showing the weakest preferential binding to proteins. Thus, the strongest protein·ligand complex is expected to form in fluoride-containing buffers, and the weakest in thiocyanide-containing buffers. Both individual K_d values and their salt concentration dependence can yield information on the extent of anion binding to a protein.

Varying the anion type, while keeping the cation type constant, can reveal if anion binding by a protein contributes to an equilibrium dissociation constant (*85*). To determine if anion binding to RNase A contributes significantly to values of K_d for complex formation in NaCl-containing buffers, we assayed the binding of Fl∼d(AUAA) to wild-type RNase A in NaF-containing buffers at four [Na^+]. We

find that the values of K_d for Fl∼d(AUAA) binding to RNase A are smaller in NaF-containing buffers for all but the binding experiment performed at the lowest [Na^+] (Table 3). At this low [Na^+], the values of K_d are 1.1 μM for binding in NaF-containing buffer and 0.82 μM for binding in NaCl-containing buffer. These values are within error of each other. The values of K_d, plotted on a logarithmic scale versus log[Na^+] in Figure 7, show only a slightly weaker dependence on NaF concentration ($\partial \log K_d/\partial \log [Na^+] = 2.0 \pm 0.2$) than on NaCl concentration ($\partial \log K_d/\partial \log [Na^+] = 2.3 \pm 0.1$). We conclude that there is only a small contribution from anion binding to wild-type RNase A under the solution conditions investigated herein. Thus, the binding of Fl∼d(AUAA) to wild-type RNase A and (we presume) the three variants show differences in their salt concentration dependence due to Coulombic interactions between residues 7, 10, and 66 and phosphoryl groups of the nucleic acid, and not because of differential anion release from the protein upon nucleic acid binding.

Contributions of the P0 and P2 Subsites to Catalysis. The function of the P0 and P2 subsites of RNase A is to contribute to both ground-state and transition-state stabilization during catalysis. Using eq 1 and the values of K_d for Fl∼d(AUAA) binding to the wild-type and K66A proteins (at conditions similar to those used for assaying catalysis), we find that the P0 subsite contributes 0.92 kcal/mol toward the binding of Fl∼d(AUAA). From a similar analysis with the K7A/R10A variant, we find that the P2 subsite contributes 1.21 kcal/mol toward the binding of Fl∼d(AUAA). The contributions from the P0 and P2 subsites to transition-state binding of poly(C) are 0.70 and 2.46 kcal/mol, respectively (Figure 4). Thus, the P0 subsite makes a uniform contribution toward binding the ground state and the transition state, whereas the P2 subsite differentiates, binding more tightly to the transition state than to the ground state. The energetic contributions of the P0 and P2 subsites to ground-state binding are similar to those of the active-site histidine residues [His12 contributes 1.5 kcal/mol and His119 contributes 1.8 kcal/mol to ground-state binding (*86*)], but far from the contribution to transition-state stabilization from either active-site histidine residue (6 kcal/mol) (*87*) or the active-site lysine residue (6.8 kcal/mol) (*88*). The P0 and P2 subsites, though distant from the active site of RNase A and contributing a relatively small amount toward transition-state stabilization, play a relatively large role in ground-state binding.

Why does the P2 subsite make a larger contribution to ground-state and transition-state binding than does the P0 subsite? The P2 subsite is comprised of two cationic residues, Lys7 and Arg10, whereas the P0 subsite contains only one cationic residue, Lys66. The presence of two positive charges may result in the release of more cations from the nucleic acid upon binding, thereby increasing the entropy more so than does the presence of a single positive charge. In addition, the B1 subsite binds nucleotides more tightly than does the B2 subsite or the B3 subsite. A pyrimidine base bound in the B1 subsite might provide an anchor for the phosphoryl group bound in the P0 subsite, providing additional binding energy that the P2 subsite must alone provide. Alternatively, another subsite beyond the P0 subsite might serve as an anchor, interacting with the phosphoryl group of the next nucleotide. Indeed, preliminary data suggest that the side chain of Arg85 of RNase A contributes significantly to nucleic acid binding and may constitute a P(−1) subsite (B. M. Fisher, J. E. Grilley, and R. T. Raines, unpublished results).

Implications. Our new knowledge of the P0 and P2 subsites of RNase A brings us one step closer to understanding the energetics of catalysis by this enzyme. In addition, our findings have implications for understanding other aspects of protein−nucleic acid interactions. For example, several restriction endonucleases rely on linear diffusion to locate their target site (*89*−*91*). By diffusing along DNA in a nonspecifically bound state, these enzymes locate target sites at rates greater than the limit set by three-dimensional diffusion (*92*). Likewise, we demonstrated recently that RNase A can use one-dimensional diffusion along a single-stranded nucleic acid to locate its target site, but that this routing is made inaccessible by added salt (*59*). This result, along with those herein, suggests that nonspecific binding is likely to rely on Coulombic interactions between the protein and nucleic acid (*93*).

ACKNOWLEDGMENT

We thank Drs. Catherine A. Royer and Paula K. Wittmayer for advice and assistance in the use of fluorescence anisotropy, Drs. M. Thomas Record, Jr. and Ruth M. Saecker for invaluable suggestions and advice on the salt concentration dependence of protein−nucleic acid interactions, and Bradley R. Kelemen, June M. Messmore, Chiwook Park, and Dr. L. Wayne Schultz for helpful discussions and comments on this manuscript.

REFERENCES

1. Steitz, T. A. (1993) *Structural Studies of Protein−Nucleic Acid Interaction: The Sources of Sequence-Specific Binding*, Cambridge University Press, Cambridge, UK.
2. Nagai, K., and Mattaj, I. W., Eds. (1994) *RNA−Protein Interactions*, Oxford University Press, Oxford, U.K.
3. Spolar, R. S., and Record, M. T., Jr. (1994) *Science 263*, 777−784.
4. Travers, A. (1993) *DNA−Protein Interactions*, Chapman and Hall, London.
5. Mossing, M. C., and Record, M. T., Jr. (1985) *J. Mol. Biol. 186*, 295−305.
6. Taylor, J. D., and Halford, S. E. (1989) *Biochemistry 28*, 6198−6207.
7. Kuriyan, J., and O'Donnell, M. (1993) *J. Mol. Biol. 234*, 915−925.
8. Kong, X. P., Onrust, R., O'Donnell, M., and Kuriyan, J. (1992) *Cell 69*, 425−437.
9. Findlay, D., Herries, D. G., Mathias, A. P., Rabin, B. R., and Ross, C. A. (1961) *Nature 190*, 781−784.
10. Cuchillo, C. M., Parés, X., Guasch, A., Barman, T., Travers, F., and Nogués, M. V. (1993) *FEBS Lett. 333*, 207−210.
11. Thompson, J. E., Venegas, F. D., and Raines, R. T. (1994) *Biochemistry 33*, 7408−7414.
12. Aguilar, C. F., Thomas, P. J., Mills, A., Moss, D. S., and Palmer, R. A. (1992) *J. Mol. Biol. 224*, 265−267.
13. Raines, R. T. (1998) *Chem. Rev. 98*, 1045−1065.
14. Jensen, D. E., and von Hippel, P. H. (1976) *J. Biol. Chem. 251*, 7198−7214.
15. Record, M. T., Jr., Lohman, T. M., and De Haseth, P. (1976) *J. Mol. Biol. 107*, 145−158.
16. McPherson, A., Brayer, G., Cascio, D., and Williams, R. (1986) *Science 232*, 765−768.
17. Birdsall, D. L., and McPherson, A. (1992) *J. Biol. Chem. 267*, 22230−22236.

18. Fontecilla-Camps, J. C., de Llorens, R., le Du, M. H., and Cuchillo, C. M. (1994) *J. Biol. Chem. 269*, 21526−21531.
19. Nogués, M. V., Vilanova, M., and Cuchillo, C. M. (1995) *Biochim. Biophys. Acta 1253*, 16−24.
20. Katoh, H., Yoshinaga, M., Yanagita, T., Ohgi, K., Irie, M., Beintema, J. J., and Meinsma, D. (1986) *Biochim. Biophys. Acta 873*, 367−371.
21. Rushizky, G. W., Knight, C. A., and Sober, H. A. (1961) *J. Biol. Chem. 236*, 2732−2737.
22. Irie, M., Watanabe, H., Ohgi, K., Tobe, M., Matsumura, G., Arata, Y., Hirose, T., and Inayama, S. (1984) *J. Biochem. (Tokyo) 95*, 751−759.
23. Tarragona-Fiol, A., Eggelte, H. J., Harbron, S., Sanchez, E., Taylorson, C. J., Ward, J. M., and Rabin, B. R. (1993) *Protein Eng. 6*, 901−906.
24. delCardayré, S. B., and Raines, R. T. (1994) *Biochemistry 33*, 6031−6037.
25. delCardayré, S. B., Thompson, J. T., and Raines, R. T. (1994) in *Techniques in Protein Chemistry V* (Crabb, J. W., Ed.) pp 313−320, Academic Press, San Diego, CA.
26. delCardayré, S. B., and Raines, R. T. (1995) *J. Mol. Biol. 252*, 328−336.
27. Parés, X., Llorens, R., Arus, C., and Cuchillo, C. M. (1980) *Eur. J. Biochem. 105*, 571−579.
28. Boqué, L., Gràcia Coll, M., Vilanova, M., Cuchillo, C. M., and Fita, I. (1994) *J. Biol. Chem. 269*, 19707−19712.
29. Parés, X., Nogués, M. V., de Llorens, R., and Cuchillo, C. M. (1991) *Essays Biochem. 26*, 89−103.
30. Richardson, R. M., Parés, X., and Cuchillo, C. M. (1990) *Biochem. J. 267*, 593−599.
31. Boix, E., Nogués, M. V., Schein, C. H., Benner, S. A., and Cuchillo, C. M. (1994) *J. Biol. Chem. 269*, 2529−2534.
32. Tartof, K. D. (1992) *Methods Enzymol. 216*, 574−584.
33. Sela, M., Anfinsen, C. B., and Harrington, W. F. (1957) *Biochim. Biophys. Acta 26*, 502−512.
34. Scopes, R. K. (1994) *Protein Purification: Principles and Practice*, Springer-Verlag, New York.
35. Kunkel, T. A., Roberts, J. D., and Zakour, R. A. (1987) *Methods Enzymol. 154*, 367−382.
36. Kim, J.-S., and Raines, R. T. (1993) *J. Biol. Chem. 268*, 17392−17396.
37. delCardayré, S. B., Ribó, M., Yokel, E. M., Quirk, D. J., Rutter, W. J., and Raines, R. T. (1995) *Protein Eng. 8*, 261−273.
38. Blank, A., Sugiyama, R. H., and Dekker, C. A. (1982) *Anal. Biochem. 120*, 267−275.
39. Ribó, M., Fernández, E., Bravo, J., Osset, M., Fallon, M. J. M., de Llorens, R., and Cuchillo, C. M. (1991) in *Structure, Mechanism and Function of Ribonucleases* (de Llorens, R., Cuchillo, C. M., Nogués, M. V., and Parés, X., Eds.) pp 157−162, Universitat Autónoma de Barcelona, Bellaterra, Spain.
40. Kim, J.-S., and Raines, R. T. (1993) *Protein Sci. 2*, 348−356.
41. Layne, E. (1957) *Methods Enzymol. 3*, 447−454.
42. Hermans, J. J., and Scheraga, H. A. (1961) *J. Am. Chem. Soc. 83*, 3283−3292.
43. Pace, C. N., Shirley, B. A., and Thomson, J. A. (1989) in *Protein Structure* (Creighton, T. E., Ed.) pp 311−330, IRL Press, New York.
44. Eberhardt, E. S., Wittmayer, P. K., Templer, B. M., and Raines, R. T. (1996) *Protein Sci. 5*, 1697−1703.
45. Cleland, W. W. (1979) *Methods Enzymol. 63*, 103−138.
46. Radzicka, A., and Wolfenden, R. (1995) *Methods Enzymol. 249*, 284−312.
47. Thompson, J. E., Kutateladze, T. G., Schuster, M. C., Venegas, F. D., Messmore, J. M., and Raines, R. T. (1995) *Bioorg. Chem. 23*, 471−481.
48. Carter, P. J., Winter, G., Wilkinson, A. J., and Fersht, A. R. (1984) *Cell 38*, 835−840.
49. Horowitz, A., and Fersht, A. (1990) *J. Mol. Biol. 214*, 613−617.
50. Horowitz, A., Serrano, L., Avron, B., Bycroft, M., and Fersht, A. R. (1990) *J. Mol. Biol. 216*, 1031−1044.
51. Mildvan, A. S., Weber, D. J., and Kuliopulos, A. (1992) *Arch. Biochem. Biophys. 294*, 327−340.
52. LeTilly, V., and Royer, C. A. (1993) *Biochemistry 32*, 7753−7758.
53. Heyduk, T., Ma, Y., Tang, H., and Ebright, R. H. (1996) *Methods Enzymol. 274*, 492−503.
54. Wittmayer, P. K., and Raines, R. T. (1996) *Biochemistry 35*, 1076−1083.
55. Wallace, R. B., and Miyada, C. G. (1987) *Methods Enzymol. 152*, 432−442.
56. Attie, A. D., and Raines, R. T. (1995) *J. Chem. Educ. 72*, 119−124.
57. Fisher, B. M. (1998) Ph.D. Thesis, University of Wisconsin−Madison.
58. Walz, F. G. (1971) *Biochemistry 10*, 2156−2162.
59. Kelemen, B. R., and Raines, R. T. (1997) in *Techniques in Protein Chemistry VIII* (Marshak, D. R., Ed.) pp 565−572, Academic Press, San Diego, CA.
60. Royer, C. A., Smith, W. R., and Beechem, J. M. (1990) *Anal. Biochem. 191*, 287−294.
61. Royer, C. A., and Beechem, J. M. (1992) *Methods Enzymol. 210*, 481−505.
62. Royer, C. A. (1993) *Anal. Biochem. 210*, 91−97.
63. Kartha, G., Bello, J., and Harker, D. (1967) *Nature 213*, 862−865.
64. Heyduk, T., and Lee, J. C. (1990) *Proc. Natl. Acad. Sci. U.S.A. 87*, 1744−1748.
65. Heyduk, T., Lee, J. C., Ebright, Y. W., Blatter, E. E., Zhou, Y., and Ebright, R. H. (1993) *Nature* 548−549.
66. Sawada, F., and Irie, M. (1969) *J. Biochem. (Tokyo) 66*, 415−418.
67. Li, J. R., and Walz, F. G. (1974) *Arch. Biochem. Biophys. 161*, 227−233.
68. Mitsui, Y., Urata, Y., Torii, K., and Irie, M. (1978) *Biochim. Biophys. Acta 535*, 299−308.
69. de Llorens, R., Arús, C., Parés, X., and Cuchillo, C. M. (1989) *Protein Eng. 2*, 417−429.
70. Beintema, J. J. (1987) *Life Chem. Rep. 4*, 333−389.
71. Beintema, J. J., Schüller, C., Irie, M., and Carsana, A. (1988) *Prog. Biophys. Mol. Biol. 51*, 165−192.
72. Wlodawer, A., Anders, L. A., Sjölin, L., and Gilliland, G. L. (1988) *Biochemistry 27*, 2705−2717.
73. Beintema, J. J. (1989) *FEBS Lett. 254*, 1−4.
74. Sorrentino, S., and Libonati, M. (1994) *Arch. Biochem. Biophys. 312*, 340−348.
75. LiCata, V. J., and Ackers, G. K. (1995) *Biochemistry 34*, 3133−3139.
76. Anderson, C. F., and Record, M. T., Jr. (1995) *Annu. Rev. Phys. Chem. 46*, 657−700.
77. Zhang, W., Bond, J. P., Anderson, C. F., Lohman, T. M., and Record, M. T., Jr. (1996) *Proc. Natl. Acad. Sci. U.S.A. 93*, 2511−2516.
78. Olmsted, M. C., Anderson, C. F., and Record, M. T., Jr. (1989) *Proc. Natl. Acad. Sci. U.S.A. 86*, 7766−7770.
79. Bujalowski, W., Overman, L. B., and Lohman, T. M. (1988) *J. Biol. Chem. 263*, 4629−4640.
80. Overman, L. B., Bujalowski, W., and Lohman, T. M. (1988) *Biochemistry 27*, 456−471.
81. Ha, J.-H., Capp, M. W., Hohenwalter, M. D., Baskerville, M., and Record, M. T., Jr. (1992) *J. Mol. Biol. 228*, 252−264.
82. Overman, L. B., and Lohman, T. M. (1994) *J. Mol. Biol. 236*, 165−178.
83. Mascotti, D. P., and Lohman, T. M. (1997) *Biochemistry 36*, 7272−7279.
84. von Hippel, P. H., and Schleich, T. (1969) in *Structure and Stability of Biological Macromolecules* (Timasheff, S. N., and Fasman, G. D., Eds.) pp 417−574, Marcel Dekker, New York.
85. Relan, N. D., Jenuwine, E. S., Gumbs, O. H., and Shaner, S. L. (1997) *Biochemistry 36*, 1077−1084.
86. Thompson, J. E. (1995) Ph.D. Thesis, University of Wisconsin-Madison.
87. Thompson, J. E., and Raines, R. T. (1994) *J. Am. Chem. Soc. 116*, 5467−5468.
88. Messmore, J. M., Fuchs, D. N., and Raines, R. T. (1995) *J. Am. Chem. Soc. 117*, 8057−8060.

89. Lohman, T. M. (1986) *CRC Crit. Rev. Biochem. 19*, 191−245.
90. Jeltsch, A., Alves, J., Wolfes, H., Maass, G., and Pingoud, A. (1994) *Biochemistry 33*, 10215−10219.
91. Berkhout, B., and van Wamel, J. (1996) *J. Biol. Chem. 271*, 1837−1840.
92. von Hippel, P. H., and Berg, O. G. (1989) *J. Biol. Chem. 264*, 675−678.
93. Winter, R. B., Berg, O. G., and von Hippel, P. H. (1981) *Biochemistry 20*, 6961−6977.

BI980743L